Interference of Bose−Einstein Condensates[†]

Y. B. Band

Department of Chemistry and the Ilse Katz Center for Nano-Science, Ben-Gurion University, Beer-Sheva 84105, Israel

Received: July 2, 2008; Revised Manuscript Received: August 26, 2008

A formalism for describing the coherence and interference properties of two atomic clouds of Bose−Einstein condensates (BEC) is presented, which is applicable even in the opposite limits when the BEC clouds are initially coherent and when they are initially independent. First, we develop a mean-field theory wherein one mean-field mode is used, and then, for fragmented (i.e., independent) condensates, we use a mean-field theory with two modes. We then develop a full two-mode field theory, with a field operator composed of a sum of two terms containing matter wave mode functions ϕ_1 and ϕ_2, that multiply the destruction operators of the modes, $\hat{a}_1$ and $\hat{a}_2$. When atom−atom interactions are present and when the mode functions overlap, the matter wave mode functions ϕ_1 and ϕ_2 develop components moving to the right and left, and this results in interference fringes in the density. At the many-body level, another source of interference arises from expectation values of the form $\langle \hat{a}_i^\dagger \hat{a}_j \rangle$ with $i \neq j$, which become nonzero due to tunneling and interactions. We detail how these two sources of interference affect the density profile and the density−density correlation functions of Bose−Einstein condensates in the coherent and in the fragmented regimes.

I. Introduction

The nature of quantum gases has been of interest to physicists and chemists since the beginning of quantum mechanics.[1] Interference of matter waves in such systems can used to explore their nature.[2−13] In the first interference experiment on Bose−Einstein condensates[2] a barrier potential was adiabatically turned on in the middle of a trapped BEC so that a double-well potential resulted. Thus, the left and right wells were separated by a barrier whose height could be experimentally controlled. Upon removing the trap potentials and the barrier between them, the atoms expanded freely and overlapped. The photographs obtained (e.g., see Figures 2 and 3) show spectacular interference fringes.[2,3,6] The ground-state of the BEC in such experiments can be coherent, with each atom being described in the mean-field approximation as being in a superposition of orbitals centered at the left and right wells, or if the barriers are sufficiently high that tunneling between them is negligible, it can be fragmented. The nature of the interference in these two cases can be quite different. Another form of interference experiment involves exposing a BEC to light pulses, called Bragg pulses, which create a periodic optical potential for the atoms composing the BEC, and the coherent process of Bragg diffraction off of the periodic potential produces a splitting of the condensate with unidirectional momentum transfer.[4−6] In this case, each atom of the condensate is in a superposition of two wave packets, one having a net momentum relative to the other, $\psi(\mathbf{r}, t) = \varphi_0(\mathbf{r}, t)e^{i\mathbf{k}_0\cdot\mathbf{r}} + \varphi_1(\mathbf{r}, t)e^{i\mathbf{k}_1\cdot\mathbf{r}}$, and the density $n(\mathbf{r}, t) = |\psi(\mathbf{r}, t)|^2$ contains an interference term proportional to $\cos[(\mathbf{k}_1 - \mathbf{k}_0)\cdot\mathbf{r}]$.

At zero temperature, the simplest description of an N particle wave function of a BEC gas is given by a product of identical single-particle wave functions

$$\Psi(\mathbf{r}_1, \mathbf{r}_2, ..., \mathbf{r}_N) = \prod_{i=1}^{N} \psi(\mathbf{r}_i) \doteq [\psi(\mathbf{r})]^N \quad (1)$$

and the dynamics of entire BEC is described in terms of a single-particle wave function, $\psi(\mathbf{r}, t)$, via the nonlinear Schrödinger equation (also called the Gross−Pitaevskii equation)[14]

$$i\hbar\frac{\partial\psi}{\partial t} = \left[-\frac{\hbar^2}{2m}\nabla^2 + V_{ex} + gN|\psi(\mathbf{r}, t)^2|\right]\psi(\mathbf{r}, t) \quad (2)$$

wherein the atomic interactions are modeled in the mean-field approximation via the nonlinear term, $gN|\psi(\mathbf{r}, t)|^2$, with an interaction strength g proportional to the s-wave scattering length a_0, $g = (4\pi\hbar^2 a_0)/m$, where m is the mass of the atoms. The density of the condensate is given by $n(\mathbf{r}, t) = N|\psi(\mathbf{r}, t)|^2$. In ref 2, $N = 5 \times 10^6$ sodium ^{23}Na atoms in the $F = 1$, $m_F = -1$ ground hyperfine state were held in a 3D harmonic magnetic trap and were exposed to a blue detuned laser-light sheet, which

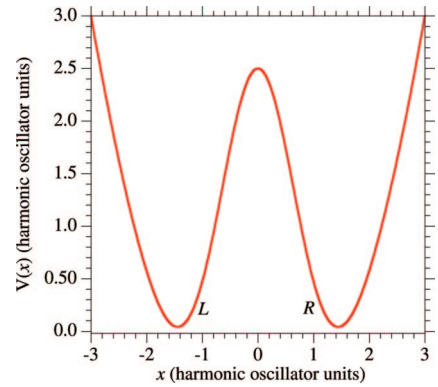

Figure 1. Double-well potential, created by applying a repulsive (blue detuned) light potential to a harmonic magnetic trapping potential, that the atoms in the BEC experience before the potential is dropped and the atoms in the BEC are allowed to freely expand.

[†] Part of the "Karl Freed Festschrift".

10.1021/jp8058195 CCC: $40.75
Published on Web 11/06/2008

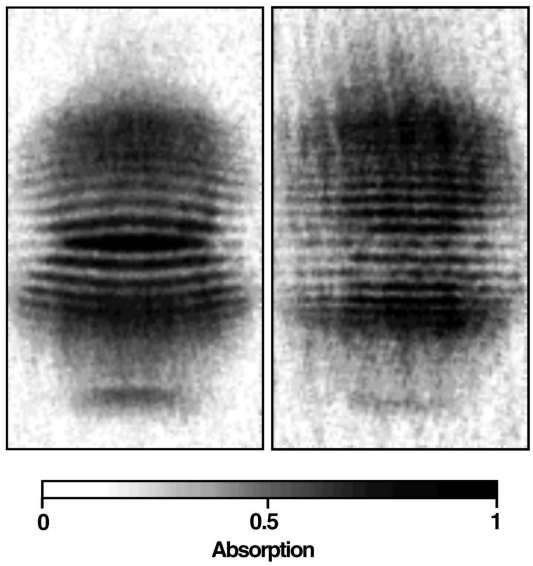

Figure 2. Interference pattern of two expanding sodium condensates observed after 40 ms free of expansion time-of-flight for two different powers of the argon ion laser-light sheet that creates a repulse potential between two parts of the condensate. The fringe periods were 20 and 15 μm, the powers were 3 and 5 mW, and the maximum absorptions were 90 and 50%, respectively, for the left and right images. The vertical axis in this figure corresponds to the horizontal axis in Figure 1. Reproduced from ref 2.

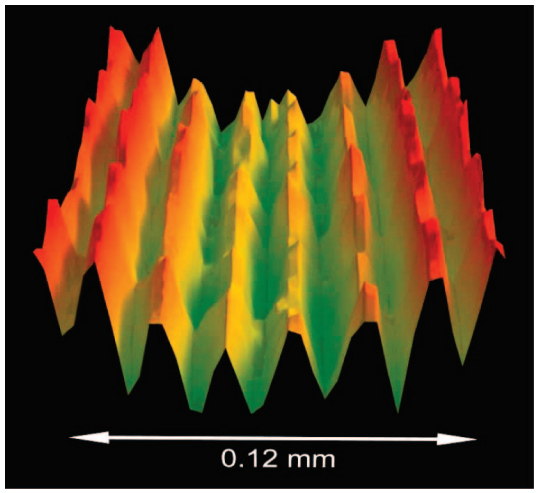

Figure 3. 3D view of the matter wave interference of two sodium BEC condensates. The projection of the sodium gas density is plotted versus position along the interference axis and the other axis perpendicular to it, and the "line-of-sight" (the same view as that in Figure 2) after the trap is removed and the gas is allowed to expand for 40 ms via free expansion. The scale of the figure is about 0.12 mm.

produced a repulsive potential so that the resulting total potential had a double-well as a function of x, and in the two perpendicular directions, the potential was a strongly confining harmonic potential, that is, $V(\mathbf{r}) = [(m\omega_x^2/2)x^2 + V_0 e^{-x^2/2\sigma^2}] + [(m\omega_y^2/2)y^2] + [(m\omega_z^2/2)z^2]$. The potential $V(x)$ is shown in Figure 1. The harmonic magnetic potential and the blue detuned laser-light sheet were then simultaneously switched off at $t = 0$, and the atoms were allowed to freely expand. Figure 2 shows the interference pattern in the measured atomic density after a 40 ms free expansion for two different strengths of the repulsive potential. Another view of the matter wave interference in the BEC density is shown in Figure 3.

The "Bragg pulse" method of producing an interference pattern in a BEC is explained in Figure 4. Two counter-

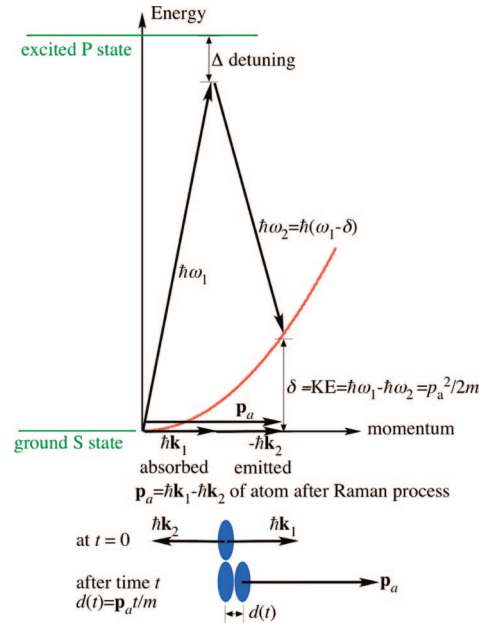

Figure 4. Phase-matching condition for Bragg pulse spectroscopy. Conservation of energy and momentum determine the conditions for two counter-propagating light pulses to create a new component of a BEC which propagates with the atomic momentum $\mathbf{p}_a = \hbar\mathbf{k}_1 - \hbar\mathbf{k}_1$. The moving wave packet will have moved a distance of $d(t) = \mathbf{p}_a t/m$ from the initial wave packet.

propagating light pulses with photon momenta $\hbar\mathbf{k}_1$ and $\hbar\mathbf{k}_2$ create a periodic potential, and if the Bragg pulses satisfy a "phase-matching" condition equivalent to conservation of the energy and momentum, atoms in the BEC scatter off of the potential to produce a momentum component $\mathbf{p}_a = \hbar\mathbf{k}_1 - \hbar\mathbf{k}_2$. The diffraction of the atoms off of the periodic potential can also be described as follows: atoms from the BEC absorb a photon from the pulse with momentum $\hbar\mathbf{k}_1$ and emit a photon into the pulse with momentum $\hbar\mathbf{k}_1$ by stimulated emission. If the photon frequencies of the Bragg pulses are ω_1 and ω_2 and their wave vectors are $\mathbf{k}_1$ and $\mathbf{k}_2$, then the momentum that the atoms obtain in the process of absorption and emission, $\mathbf{p}_a = \hbar\mathbf{k}_1 - \hbar\mathbf{k}_1$, and their kinetic energy $\mathbf{p}_a^2/2m$ satisfy the phase-matching conditions

$$\delta \equiv \hbar\omega_1 - \hbar\omega_2 = \frac{\mathbf{p}_a^2}{2m} \tag{3a}$$

$$\mathbf{p}_a = \hbar\mathbf{k}_1 - \hbar\mathbf{k}_2 \tag{3b}$$

This is a Bragg scattering process. For a condensate wave function given by $\psi(\mathbf{r}, 0) = \varphi_0(\mathbf{r}, 0)$ before the Bragg scattering, immediately after the Bragg scattering, the condensate wave function becomes $\psi(\mathbf{r}, 0) = c_0\varphi_0(\mathbf{r}, t) + c_1\varphi_0(\mathbf{r}, 0)e^{i\mathbf{p}_a\cdot\mathbf{r}/\hbar}$, where the amplitude $c_1 = (1 - c_2^2)^{1/2}$ depends on the Bragg pulse intensities and the pulse durations. After a time t, the moving wave packet will have moved a distance $d(t) = \mathbf{p}_a t/m$. Figure 5 shows the calculated density of $N = 500\,000$ sodium atoms in a harmonic trap with 84, 59, and 42 Hz immediately after the application of the Bragg pulses and 274 μs afterward. An interference pattern in the density is clearly visible.

Upon application of two sets of Bragg pulses, one can make an initial condensate with three wave packets having central momentum $\mathbf{p}_1 = 0$, $\mathbf{p}_2 = \hbar k_{ph}(\hat{\mathbf{x}} - \hat{\mathbf{y}})$, and $\mathbf{p}_3 = 2\hbar\mathbf{k}_{ph} = \hbar k_{ph}\hat{\mathbf{x}}$, as shown in Figure 6a. After some time, the three wave packets

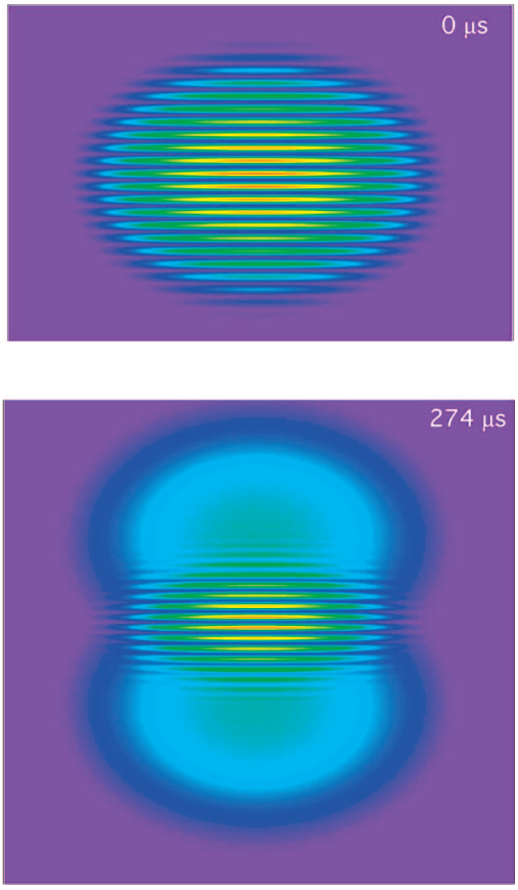

Figure 5. Interference pattern of $N = 500\,000$ sodium atoms in a harmonic trap with 84, 59, and 42 Hz immediately after the application of Bragg pulses and 274 μs afterward. The vertical axis in this figure corresponds to the horizontal axis for the condensate wave packets in Figure 4.

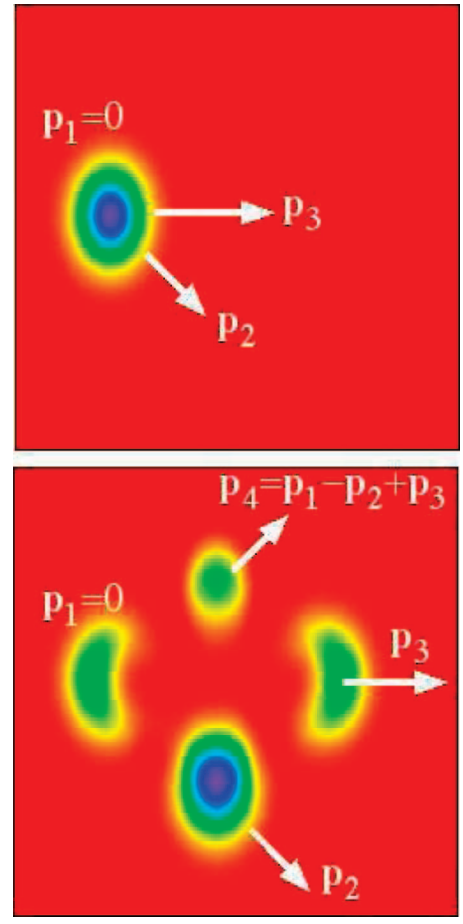

Figure 6. Four-Wave Mixing. In the top frame, the initial condensate is subjected to a set of Bragg pulses that make three coherent wave packet components, $\psi(\mathbf{r}, 0) = c_1\varphi_0(\mathbf{r}, 0)e^{i\mathbf{p}_1\cdot\mathbf{r}/\hbar} + c_2\varphi_0(\mathbf{r}, 0)e^{i\mathbf{p}_2\cdot\mathbf{r}/\hbar} + c_3\varphi_0(\mathbf{r}, 0)e^{i\mathbf{p}_3\cdot\mathbf{r}/\hbar}$. In the bottom frame, these components have produced a fourth wave with momentum $\mathbf{p}_4 = \mathbf{p}_1 - \mathbf{p}_2 + \mathbf{p}_3$, and the wave packets have separated from one another.

separate, but instead of having just three wave packets, a fourth wave packet with momentum $\mathbf{p}_4 = \mathbf{p}_1 - \mathbf{p}_2 + \mathbf{p}_3$ develops.[15,16] This process comes about from four-wave mixing. The initial state of the condensate is given by $\psi(\mathbf{r}, 0) = c_1\varphi_0(\mathbf{r}, 0)e^{i\mathbf{p}_1\cdot\mathbf{r}/\hbar} + c_2\varphi_0(\mathbf{r}, 0)e^{i\mathbf{p}_2\cdot\mathbf{r}/\hbar} + c_3\varphi_0(\mathbf{r}, 0)e^{i\mathbf{p}_3\cdot\mathbf{r}/\hbar}$, with amplitudes c_1, c_2, and c_3 that depend on the Bragg pulse intensities and the pulse durations; in Figure 6, the initial population fractions are taken to be 0.412, 0.176, and 0.412, respectively. Upon substituting this initial condition into eq 2, the nonlinear term on the right-hand side of the equation creates a wave packet with momentum $\mathbf{p}_4 = \mathbf{p}_1 - \mathbf{p}_2 + \mathbf{p}_3$, that is, the three waves in the initial condensate wave function generate the fourth wave via the nonlinear term $gN\psi^*(\mathbf{r}, t)\psi(\mathbf{r}, t)\psi(\mathbf{r}, t)$. This process can also be viewed as an interference process; wave packets 1 and 2 form an interference pattern of which packet 3 scatters off, and also, wave packets 2 and 3 form an interference pattern of which packet 1 scatters off. Figure 6b shows the wave packets in physical space some time after the Bragg pulses created the three initial waves; the four wave packets have already separated from one another.

In section II, we provide a description based upon mean-field theory of the BEC in a double-well potential and describe the interference patterns that are expected due to the interaction of the atoms in the condensate. In section III, we augment the mean-field picture by giving a field theory description of a BEC in the double-well potential and describe a new interference mechanism that contributes to the density profile of the atoms upon releasing the trap potential. Section IV concludes and summarizes the results.

II. Fragmented, Coherent, and General States of a Condensate

Let us now consider the type of states that can be formed in a double-well potential of the form shown in Figure 1. For simplicity, let us allow only two modes, ϕ_L and ϕ_R; the general form of the multiparticle wave function under this description is

$$\Psi(\mathbf{r}_1, \mathbf{r}_2, ..., \mathbf{r}_N) = c_0\phi_L^N + c_1\phi_L^{N-1}\phi_R + c_2\phi_L^{N-2}\phi_R^2 + ...+ c_{N/2}\phi_L^{N/2}\phi_R^{N/2} + ...+c_{N-1}\phi_L\phi_R^{N-1} + c_N\phi_R^N \quad (4)$$

Two limiting forms of eq 4 are the coherent state given by eq 1 with $\psi = 1/(2)^{1/2}(\phi_L + \phi_R)$, which yields amplitudes given by the binomial coefficients $\left\{c_n = \binom{N}{n}\right\}$, $n = 0, 1,..., N$, and the fragmented condensate, which has only one term in eq 4, $\Psi = c_{N/2}\phi_L^{N/2}\phi_R^{N/2}$. In the latter case, exactly $N/2$ atoms are present in each well (N must be even), whereas in the former, each condensate atom has an equal probability of being in the right and left wells.

Often in double-well interference-type experiments, atoms are prepared in a double-well trap potential, and it is not clear whether the atoms form a coherent BEC, fragmented BECs, or

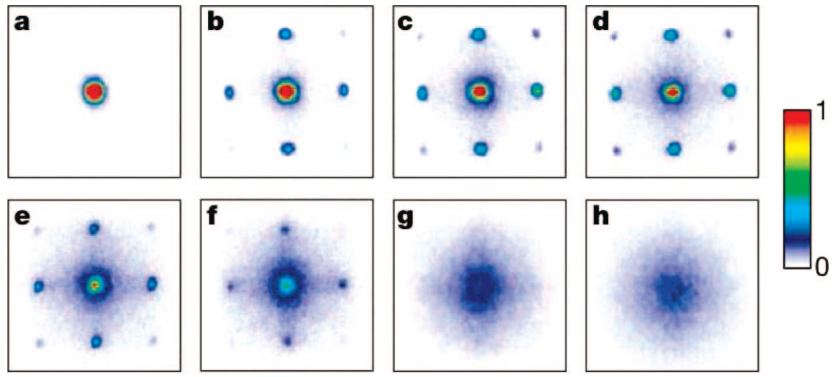

Figure 7. Phase transition from superfluid to Mott insulating regimes. Dynamical evolution of the multiple matter wave interference pattern observed for various potential trap depths from $0E_R$ to $20E_R$ (frame a has a trap depth of 0, b has $3E_R$, c has $7E_R$, d has $10E_R$, e has $13E_R$, f has $14E_R$, g has $16E_R$, and h has $20E_R$). The vanishing of the interference pattern is caused by a phase transition from a coherent state into a state where the number of atoms in each each lattice site is exactly specified (i.e., a transition from a state of the form of eq 9 to a state of the form in eq 5. Reproduced from ref 18.

a more general form of a many-body wave function of the form in eq 4. However, it is feasible to produce two spatially separated, initially independent BECs,[17] and this allows for experiments with definitely fragmented BECs. The interference pattern that results from two initially independent condensates is great interest, as is the transition from a coherent state to a fragmented state as the strength of the repulsive potential between the wells increases.

Markus Greiner and colleagues performed a series of experiments to study the nature of the degenerate quantum gas in a multiple-well optical potential.[18] They measured the momentum distribution of the condensate when it was held in a 3D periodic optical potential by suddenly releasing the atoms from the optical lattice potential (i.e., turning the optical potential off) at different potential trap depths and then taking absorption images of the atomic cloud after the cloud had expanded. The absorption images of the cloud showing the interference patterns that resulted is shown in Figure 7. As the height of the optical potential was increased, an interference pattern developed, but as the strength of the optical potential increased beyond a certain value ($16E_R$ in Figure 7, where the recoil energy is defined as $E_R = \hbar^2 k_{ph}^2/2m$), the interference pattern disappeared. This disappearance is a zero temperature phase transition from a superfluid phase of the condensate to a Mott insulator phase. The dimensionless parameter used in describing the transition is the ratio of the tunneling rate from well to well to the nonlinear interaction strength which is proportional to g.[19] The phase coherence of the condensate can be restored from the Mott insulator state when the optical potential is lowered again to a value where the ground state of the many-body system is completely superfluid. Upon reversing the potential depth from $20E_R$ back down to $0E_R$, there is a revival of the interference pattern.

Without atom−atom interaction, there cannot be interference in the expectation value of the density operator for a state that is well described as a product of number states of the two initially isolated ultracold clouds in the double-well potential. For any such initial state given by a product of number states

$$|\Psi_0\rangle \sim (\hat{a}_L^\dagger)^{N_L}(\hat{a}_R^\dagger)^{N_R}|0\rangle \tag{5}$$

the interference term in the density vanishes, as we shall now explicitly show. The density $n(\mathbf{r}, t)$ at position $\mathbf{r}$ at time t is given by the expectation value of the density operator $\hat{n}(\mathbf{r}, t) = \hat{\psi}^\dagger(\mathbf{r}, t)\hat{\psi}(\mathbf{r}, t)$

$$n(\mathbf{r}, t) = \langle\Psi_0|\hat{\psi}^\dagger(\mathbf{r}, t)\hat{\psi}(\mathbf{r}, t)|\Psi_0\rangle \tag{6}$$

Here, the field operator $\hat{\psi}$ for the condensate can expanded in terms of the mode functions ϕ_i

$$\hat{\psi}(\mathbf{r}, t) = \hat{a}_L\phi_L(\mathbf{r}, t) + \hat{a}_R\phi_R(\mathbf{r}, t) \tag{7}$$

Substituting the field operator (eq 7) and the number state (eq 5) into the formula in eq 6 for the expectation value, we get

$$n(\mathbf{r}, t) = \langle\Psi_0|(\sum_{i=L,R} \hat{a}_i^\dagger\hat{a}_i|\phi_i(\mathbf{r}, t)|^2) + (\hat{a}_R^\dagger\hat{a}_L\phi_R^\dagger(\mathbf{r}, t)\phi_L(\mathbf{r}, t) + \text{h.c.})|\Psi_0\rangle \tag{8}$$

The interference terms on the right-hand side of eq 8 vanish, irrespective of the nature of the basis functions $\phi_i(\mathbf{r}, t)$, since $\langle\Psi_0|\hat{a}_R^\dagger\hat{a}_L|\Psi_0\rangle$ and $\langle\Psi_0|\hat{a}_L^\dagger\hat{a}_R|\Psi_0\rangle$ vanishes for states $|\Psi_0\rangle$, which are a product form such as that in eq 5. This completes the proof. In contrast, for an initial state given by a product of coherent states

$$|\tilde{\Psi}_0\rangle \sim \left[\frac{1}{\sqrt{2}}(\hat{a}_L^\dagger + \hat{a}_R^\dagger)\right]^N|0\rangle \tag{9}$$

interference terms proportional to $\langle\Psi_0|\hat{a}_R^\dagger\hat{a}_L|\Psi_0\rangle$ would be present. Therefore, without atom−atom interaction, we expect the initially fragmented state not to have interference fringes but the coherent state to have interference.[20]

However, for interacting atoms (i.e., for nonvanishing g), the first term on the right-hand side of eq 8 can yield an interference pattern, as we shall now see. We use a multiorbital mean-field theory[21,22] to determine the orbitals for fragmented states. For two modes, this will be similar to a two-orbital approximation for an excited state of helium, but here, many bosons can occupy a given orbital; no Pauli exclusion principle applies to bosonic particles. For a double-well potential, the two-orbital time-dependent mean-field equations take the form of[23]

$$i\dot{\phi}_L = \mathscr{P}[\hat{h} + \lambda(N_L - 1)|\phi_L|^2 + 2\lambda N_R|\phi_R|^2]\phi_L \quad (10a)$$

$$i\dot{\phi}_R = \mathscr{P}[\hat{h} + \lambda(N_R - 1)|\phi_R|^2 + 2\lambda N_L|\phi_L|^2]\phi_R \quad (10b)$$

and initial conditions $\phi_{L,R}(x, t = 0)$ are necessary to begin propagation of these equations. The operator $\hat{h}$ is the usual one-particle Hamiltonian, and $\mathscr{P} = 1 - |\phi_L\rangle\langle\phi_L| - |\phi_R\rangle\langle\phi_R|$ is a projector that ensures orthonormalization of the orbitals ϕ_L and ϕ_R. The last two terms on the right-hand side of eqs 10a and 10b are the self and cross mean-field interaction terms, and the parameter λ is proportional to the interaction strength parameter g. Note the factor of 2 in the cross mean-field interaction terms; the cross mean-field is twice as strong as the self mean-field, in a fashion similar to BEC wave packet collisions,[24] two-component (or more) BEC theories,[25] and optical pulse interactions.[26] In two-mode time-dependent mean-field, the density is expressed by $n(x, t) = N_L|\phi_L(x, t)|^2 + N_R|\phi_R(x, t)|^2$ (see the first term on the right-hand side of eq 8). Since we are interested in propagating the orbitals after the external potential is dropped, in our scenario, $\hat{h}$ is just the kinetic energy operator $-(1/2m)(\partial^2/\partial x^2)$.

Figure 8 shows the calculated density as a function of time after the external potential is dropped, given an initial fragmented condensate with 500 atoms in each well with densities centered at the well minima, $\pm x_0$ with $x_0 = 6$ for $\lambda = 0.1$. At about $t = 3$, one begins to see impact of the interference term in the density, which becomes strongly pronounced as time proceeds. For comparison, we plot the solution to the (one-mode) Gross−Pitaevskii equation (in red), which does not show interference fringes. We conclude that the density of two initially independent (fragmented) condensates which begin to overlap can show interference effects due to interparticle interaction.

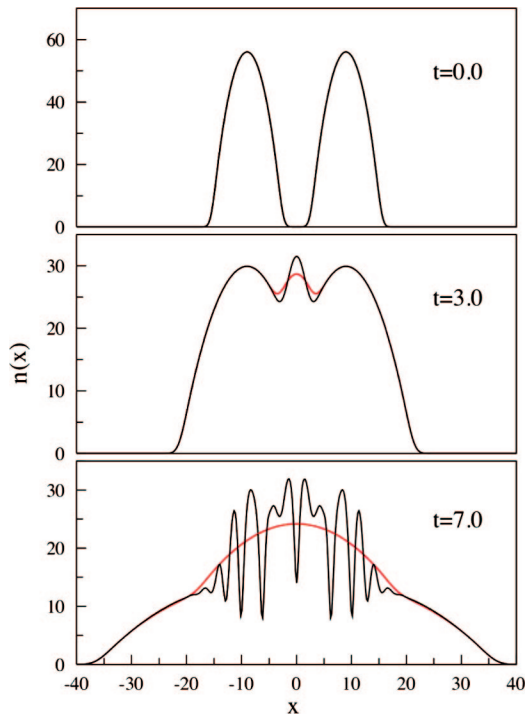

Figure 8. The density $n(x, t)$ of two condensates of 500 atoms each for $\lambda = 0.1$ as a function of time computed with two-mode time-dependent mean-field (black) compared to the density $n_{LL} + n_{RR}$ of two BECs which do not interact with each other, each computed with the Gross−Pitaevskii equation (red). The quantities shown are dimensionless.

The interference fringes appearing in Figure 8 are simple to interpret. Atoms in the ϕ_L wave packet encounter the mean-field potential resulting from the repulsive interactions with the atoms in wave packet ϕ_R, and wave packet ϕ_L thereby begins to develop a right-moving component in the overlap region of ϕ_R and ϕ_L. Since both right- and left-moving components are present in ϕ_L in the overlap region, an interference pattern appears in the density $|\phi_R|^2$ in the overlap region. This is just like the scattering of a wave packet of left-moving particles hitting a wall positioned to its right; the interaction with the wall will reflect the particles, and the wave packet near the wall develops both right- and left-moving components, so that an interference pattern results in the particle density near the wall. Similarly, the atoms in mode ϕ_R encounter the potential resulting from the repulsive interactions with the atoms in mode ϕ_L, and the density $|\phi_L|^2$ also develops an interference pattern. The densities $|\phi_L|^2$ and $|\phi_R|^2$ can now be substituted into the first term on the right-hand side of eq 8, which yield the total density $n(\mathbf{r}, t)$ if the second term on the right-hand side vanishes.

In the next section, we shall see that a new mechanism for interference arises for the fragmented condensate initial state, via the second term on the right-hand side of eq 8. This mechanism is not accounted for in the two-mode time-dependent mean-field description. It results due to quantum tunneling and interaction.

III. Two-Mode Field Theory

The many-body field theory description of the condensate begins by writing out the Hamiltonian of the system of bosons. Taking the interaction in the form of a point contact interaction, since the size of the condensate is so much bigger than the scale of the atom−atom interaction, gives

$$H = \int d\mathbf{r}\hat{\psi}^\dagger(\mathbf{r})\left[H_0(\mathbf{r}, t) + \frac{1}{2}g\hat{\psi}^\dagger(\mathbf{r})\hat{\psi}(\mathbf{r})\right]\hat{\psi}(\mathbf{r}) \quad (11)$$

where $H_0(\mathbf{r}, t) = p^2/2m + V(\mathbf{r}, t)$. We expand the field operator $\hat{\psi}(\mathbf{r}, t)$ at any given time in terms of the orthogonal orbital functions $\phi_j(\mathbf{r}, t)$ and the annihilation operators $\hat{a}_j$ for atoms in internal state j, where $j = L, R$

$$\hat{\psi}(\mathbf{r}, t) = \sum_{j=L,R} \phi_j(\mathbf{r}, t)\hat{a}_j \quad (12)$$

where at any time $\int d\mathbf{r}\phi_j^*(\mathbf{r}, t)\phi_k(\mathbf{r}, t) = \delta_{jk}$ and the operators $\hat{a}_j$ obey $[\hat{a}_j, \hat{a}_k^\dagger] = \delta_{jk}$. The Hamiltonian therefore takes the form

$$\hat{H} = \sum_{i=L,R} E_i\hat{a}_i^\dagger\hat{a}_i - \frac{\hbar\Omega}{2}(\hat{a}_L^\dagger\hat{a}_L + \hat{a}_R^\dagger\hat{a}_L) + \sum_{i,j=L,R} G_{ij}\hat{a}_i^\dagger\hat{a}_j^\dagger\hat{a}_j\hat{a}_i \quad (13)$$

where the parameters E_i, Ω, and G_{ij} corresponding to the energy on each well, the tunneling rate between wells, and the atom−atom interaction parameters for atoms in the right and left wells (G_{ii}) and cross interaction of atoms in the right well and left well (G_{ij}) can be obtained in terms of integrals over the mode functions.

The expectation value of the density operator, $n \equiv \langle\hat{n}\rangle = \langle\hat{\psi}^\dagger\hat{\psi}\rangle$, contains the term $\langle\hat{a}_L^\dagger\hat{a}_R\rangle$; see eq 8. For an initially fragmented condensate, $\langle\hat{a}_L^\dagger\hat{a}_R\rangle_{t=0} = 0$, but as the mode functions begin to overlap, $\langle\hat{a}_L^\dagger\hat{a}_R\rangle$ will begin to deviate from zero. The calculation of the expectation value $\langle\hat{a}_L^\dagger\hat{a}_R\rangle$ was carried out by

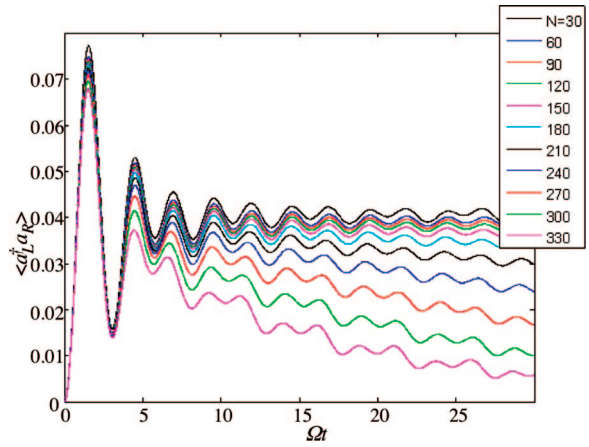

Figure 9. $\langle \hat{a}_L^\dagger \hat{a}_R \rangle$ versus time for an initially fragmented condensate.

using an angular momentum representation,[27] wherein one defines the number operators as

$$\hat{n}_i = \hat{a}_i^\dagger \hat{a}_i \qquad \hat{N} = \hat{n}_L + \hat{n}_R \tag{14}$$

and the angular momentum operators as

$$\hat{L}_z = \frac{\hat{n}_L - \hat{n}_R}{2} \qquad \hat{L}_x = \frac{\hat{a}_L^\dagger \hat{a}_R + \hat{a}_R^\dagger \hat{a}_L}{2}$$

$$\hat{L}_y = \frac{\hat{a}_L^\dagger \hat{a}_R - \hat{a}_R^\dagger \hat{a}_L}{2i} \tag{15}$$

so that the Hamiltonian can be written as

$$\hat{H} = E\hat{N} + \hbar\Delta\hat{L}_z - \hbar\Omega\hat{L}_x + \sum_{i=1}^{2} G_{ii}(\hat{n}_i^2 - \hat{n}_i) + 2G_{LR}\hat{n}_L\hat{n}_R \tag{16}$$

where the parameters are $E \equiv (E_L + E_R)/2$ and $\hbar\Delta \equiv (-E_R + E_L)$. Since $\hat{N}$ commutes with $\hat{H}$, the Hamiltonian conserves the total number of particles. Using the identities $\hat{n}_L = \hat{N}/2 + \hat{L}_z$ and $\hat{n}_R = \hat{N}/2 - \hat{L}_z$, we obtain the Hamiltonian

$$\hat{H} = \left(E - \frac{G_{LL} + G_{RR}}{2}\right)\hat{N} + (G_{LL} + G_{RR} + 2G_{LR})\frac{\hat{N}^2}{4} - \hbar\Omega\hat{L}_x + [\hbar\Delta + (G_{LL} - G_{RR})(\hat{N} - 1)]\hat{L}_z + (G_{LL} + G_{RR} - 2G_{LR})\hat{L}_z^2 \tag{17}$$

The initial fragmented state can be written as $|\Psi_0\rangle = |L = N, L_z = 0\rangle \equiv |N_L = N/2, N_R = N/2\rangle$, and the expectation value $\langle \hat{a}_L^\dagger \hat{a}_R \rangle_t$ can be written as

$$\langle \hat{a}_L^\dagger \hat{a}_R \rangle_t \equiv \langle \hat{a}_L^\dagger(t)\hat{a}_R(t) \rangle = \langle \Psi_0 | (L_x(t) + iL_y(t)) | \Psi_0 \rangle \tag{18}$$

in the Heisenberg representation or $\langle \Psi_0(t)|(L_x + iL_y)|\Psi_0(t)\rangle$ in the Schrödinger representation.

Figure 9 shows the calculated values of $\langle \hat{a}_L^\dagger \hat{a}_R \rangle_t$ versus time for an initially fragmented condensate. At $t = 0$, the expectation value $\langle \Psi_0|(L_x + iL_y)|\Psi_0\rangle_{t=0} = \langle \Psi_0|\hat{a}_R^\dagger \hat{a}_L|\Psi_0\rangle_{t=0}$ is zero for an initial fragmented state, but due to quantum tunneling and interaction, the expectation value $\langle \Psi_0|(L_x + iL_y)|\Psi_0\rangle_t = \langle \Psi_0|\hat{a}_R^\dagger \hat{a}_L|\Psi_0\rangle_t$ becomes finite for times $t > 0$. Hence, another mechanism for the density to develop interference fringes arises from the $\langle \hat{a}_L^\dagger \hat{a}_R \rangle$ term in eq 8 due to the quantum tunneling term in the Hamiltonian and due to interactions.

IV. Summary and Conclusion

Interference of condensates can be used to probe correlation functions of degenerate gaseous systems, not just their order parameter and their density distribution. In other words, interference fringes observed in condensate experiments are strongly affected by atom−atom interactions and can therefore be used to tell us about the correlations in a degenerate quantum gas.

Here, we discussed a number of different ways that interference arises in BEC experiments, including release of a BEC from a double-well potential, Bragg pulse experiments where two or more BEC components with different central momenta are created, and four-wave mixing wherein a fourth wave is created from three waves via scattering off of interference patterns made by BEC components with different momenta. We have explored two opposite limits of the interference from a BEC in a double-well potential, the initially coherent and the initially independent (fragmented) cases. We developed a mean-field theory using two modes and compared it with the one-mode Gross−Pitaevskii treatment. We then developed a full two-mode field theory and showed that an additional mechanism for interference fringes exists and results due to quantum tunneling and interaction.

A degenerate Bose gas can behave very differently in 1D, 2D, and 3D. For example, in 2D, a proliferation of thermal vortices at finite temperature can cause a Berezinskii–Kosterlitz–Thouless phase transition, and at finite temperatures, thermal fluctuations can destroy long-range order, and this directly affects the interference fringes.[28] We have not directly addressed these issues here within the context of the simple model systems presented.

We should also mention that in a given experiment, the density pattern observed is not the expectation value of the density operator.[8] For example, for the fragmented initial state and without interaction, fringes in a particular experiment would still appear in a given experiment but would be seen with a different random phase at each given realization of the experiment. If one then averages the fringe pattern over many experiments, we would get zero interference in the density if no interactions are present. We could calculate the density−density correlation function, $\langle \hat{n}(\mathbf{r}, t)\hat{n}(\mathbf{r}', t) \rangle$, in the expanded cloud, and this would give a measure of the fluctuations in the density. The correlation function does have an oscillating part, even without interactions present, and the fringe amplitude does not fluctuate in the correlation function. When interactions are present, a deterministic interference in the density is also present; therefore, both a random, fluctuating component and a deterministic component of the interference would be present in a given experiment (of course, upon averaging over many such single experiments, only the deterministic component would survive and would correspond to the expectation value of the density operator). Explicit calculations of both the density and the density correlation functions using the full two-mode field theory will be presented in future publications.

References and Notes

(1) (a) Huang, K. *Statistical Mechanics*; John Wiley: New York, 1987. (b) Rice, S. A.; Freed, K. F.; Light, J. C. *Statistical Mechanics: New*

Concepts, New Problems, New Applications; University Chicago Press: Chicago, IL, 1972. My first exposure to the treatment of quantum gases came in a course that Karl Freed taught in 1971 at the University of Chicago on statistical mechanics; the course included such topics as Liouville's theorem, the BBGKY hierarchy, and Chapman−Enskog expansions.

(2) Andrews, M. R.; et al. *Science* **1997**, *275*, 637.

(3) Schumm, T.; et al. *Nat. Phys.* **2005**, *1*, 57.

(4) Kozuma, M.; et al. *Phys. Rev. Lett.* **1999**, *82*, 871.

(5) Stenger, J.; et al. *Phys. Rev. Lett.* **1999**, *82*, 4569.

(6) Hagley, E. W.; et al. *Phys. Rev. Lett.* **1999**, *83*, 3112.

(7) Naraschewski, M.; et al. *Phys. Rev. A* **1996**, *54*, 2185.

(8) Javanainen, J.; Yoo, S. M. *Phys. Rev. Lett.* **1996**, *76*, 161.

(9) Castin, Y.; Dalibard, J. *Phys. Rev. A* **1997**, *55*, 4330.

(10) Hegstrom, R. A. *Chem. Phys. Lett.* **1998**, *288*, 248.

(11) Leggett, A. J. *Rev. Mod. Phys.* **2001**, *73*, 307.

(12) Röhrl, A.; et al. *Phys. Rev. Lett.* **1997**, *78*, 4143.

(13) Liu, W.-M.; Wu, B.; Niu, Q. *Phys. Rev. Lett.* **2000**, *84*, 2294.

(14) (a) Gross, E. P. *Nuovo Cimento* **1961**, *20*, 454. (b) Gross, E. P. *J. Math. Phys.* **1963**, *4*, 195. (c) Pitaevskii, L. P. *Zh. Eksp. Teor. Fiz.* **1961**, *40*, 646. [*Sov. Phys. JETP* **1961**, *13*, 451]

(15) Trippenbach, M.; Band, Y. B.; Julienne, P. *Opt. Express* **1998**, *3*, 530.

(16) Deng, L.; et al. *Nature* **1999**, *398*, 218.

(17) Shin, Y.; et al. *Phys. Rev. Lett.* **2005**, *95*, 170402.

(18) Greiner, M.; et al. *Nature* **2002**, *419*, 51.

(19) Fisher, M. P. A.; Weichman, P. B.; Grinstein, G.; Fisher, D. S. *Phys. Rev. B* **1989**, *40*, 546.

(20) It should be noted that what one sees in one experiment may not be the expectation value of the density. For a particular experiment, the interference fringes might appear with a random phase, and if an average over many experiments is performed, the fringe pattern over many experimental outcomes would average to zero if no interactions were present for the case of a fragmented initial state.

(21) (a) Streltsov, A. I.; et al. *Phys. Rev. A* **2004**, *70*, 053607. (b) Alon, O. E.; Cederbaum, L. S. *Phys. Rev. Lett.* **2005**, *95*, 140402. (c) Alon, O. E.; et al. *Phys. Lett. A* **2007**, *362*, 453.

(22) Cederbaum, L. S.; Streltsov, A. I.; Band, Y. B.; Alon, O. E. *Phys. Rev. Lett.* **2007**, *98*.

(23) Written out explicitly, these equations take the form

$$i\dot{\phi}_L = [\hat{h} + \lambda(N_L - 1)|\phi_L|^2 + 2\lambda N_R|\phi_R|^2]\phi_L - \langle\phi_L|[\hat{h} + \lambda(N_L - 1)|\phi_L|^2 + 2\lambda N_R|\phi_R|^2]|\phi_L\rangle\phi_L - \langle\phi_R|[\hat{h} + \lambda(N_L - 1)|\phi_L|^2 + 2\lambda N_R|\phi_R|^2]|\phi_L\rangle\phi_R \quad (19a)$$

$$i\dot{\phi}_R = [\hat{h} + \lambda(N_R - 1)|\phi_R|^2 + 2\lambda N_L|\phi_L|^2]\phi_R - \langle\phi_L|[\hat{h} + \lambda(N_L - 1)|\phi_L|^2 + 2\lambda N_R|\phi_R|^2]|\phi_R\rangle\phi_L - \langle\phi_R|[\hat{h} + \lambda(N_L - 1)|\phi_L|^2 + 2\lambda N_R|\phi_R|^2]|\phi_R\rangle\phi_R \quad (19b)$$

(24) Trippenbach, M.; Band, Y. B.; Julienne, P. S. *Phys. Rev. A* **2000**, *62*, 023608.

(25) Burke, J. P.; Julienne, P. S.; Williams, C. J.; Band, Y. B.; Trippenbach, M. *Phys. Rev. A* **2004**, *70*, 033606.

(26) Radzewicz, C.; Band, Y. B.; Pearson, G. W.; Krasinski, J. S. *Opt. Commun.* **1995**, *117*, 295.

(27) (a) Band, Y. B.; Vardi, A. *Phys. Rev. A* **2006**, *74*. (b) Band, Y. B.; Vardi, A. *Laser Phys.* **2008**, *18*, 308.

(28) Hadzibabic, Z.; Kruger, P.; Cheneau, M.; Battelier, B.; Dalibard, J. *Nature* **2006**, *441*, 1118.

JP8058195